line shapes under these conditions will be the line shape due to nonorientation-dependent broadening and may be used to deconvolute reorientational correlation functions from spectral bands observed under different conditions. The results of line-shape[15,20] and line-width[7] studies suggest that this may be possible. By using this technique, information about additional components of the anisotropic reorientational motion in the liquid phase would be available.

In addition to providing an excellent tool for the study of the liquid state, the method we have described can also be of use to chemists with more diverse interests. As Gordon[34] has pointed out, reorientational correlation times obtained from Raman line shapes can be used with nmr relaxation times to determine molecular properties. As can be seen in eq 28, a knowledge of the nmr spin-lattice relaxation time T_1 and the reorientational correlation time τ_{20} allows us to determine the nuclear quadrupole coupling constant for deuterium in *d*-chloroform. The value, we determine, for the nuclear quadrupole coupling constant is $(eqQ/h) = 0.174$ MHz, which compares quite favorably with a value of $(eqQ/h) = 0.168$ MHz determined from nqr measurements on solid *d*-chloroform.[35] This result is encouraging and suggests the wider importance of this method.

Acknowledgments. The authors wish to acknowledge the partial support of this research by the National Science Foundation through US NSF GP 31431X. The authors wish to thank Professor M. V. Klein and the Materials Research Laboratory of the University of Illinois for their help and the use of their Raman spectrometer.

(34) R. G. Gordon, *J. Chem. Phys.*, **42**, 3658 (1965).

(35) J. L. Ragle and K. L. Sherk, *ibid.*, **50**, 3553 (1969).

A Semicontinuum Model for Trapped Electrons in Polar Liquids and Solids. Trends with Matrix Polarity

K. Fueki,[1] D.-F. Feng, and Larry Kevan*

Contribution from the Department of Chemistry, Wayne State University, Detroit, Michigan 48202. *Received September 6, 1972*

Abstract: A semicontinuum model is extended to trapped electrons in 2-methyltetrahydrofuran glass and in three amine glasses at 77°K. It is shown to account for recent experimental results quite well. The semicontinuum model has also been modified for trapped electrons in aqueous glasses like 10 *M* NaOH by neglecting long-range polarization interactions. This modification successfully predicts no bound excited state in agreement with experiment. Revised calculations are given for electrons in water and ice and configuration coordinate diagrams are presented for the above matrices and for electrons in liquid and glassy methanol and ethanol. The effects of the various physical constants of the matrices on the trapped electron energy level structure is discussed from the viewpoint of matrix polarity.

One of the surprising and generally significant findings of radiation chemical studies in the last decade has been the discovery of solvated and trapped electrons as distinct chemical entities in a variety of liquids and glassy solids.[2,3] These species have typical lifetimes of microseconds in room temperature liquids and seem indefinitely stable in many glassy solids at 77°K. All of these electrons are characterized by a strong absorption spectrum in the visible or infrared regions. Early theoretical studies were oriented toward accounting for the absorption spectrum of solvated electrons in water and liquid ammonia.[4-8] The electron cavity radius was used as a parameter to fit the energy of the absorption maximum to the calculated energy difference between the ground and first excited states. In more recent theoretical work a semicontinuum model has been developed by which the configurational stability of the ground state of the electrons has been determined in water and ice,[9] and in methanol and ethanol.[10,11] The configurational stability of electrons in liquid ammonia has also been established by a slightly different method of calculation.[12] In the semicontinuum model the cavity radius is no longer a parameter, but the energy of the electron in the quasi-free electron state or conduction state, V_0, does remain as a limited (between -1 and 1 eV) parameter. However, V_0 seems amenable to experimental measurement.[13]

Recent experimental work on electrons in several glassy matrices[14-16] and in crystalline ice[16,17] at 77°K

(1) On leave from Nagoya University, Nagoya, Japan.

(2) E. J. Hart and M. Anbar, "The Hydrated Electron," Wiley-Interscience, New York, N. Y., 1970.

(3) (a) L. Kevan, *Actions Chim. Biol. Radiat.*, **13**, 57 (1969); (b) *ibid.*, **15**, 81 (1971).

(4) J. Jortner, *J. Chem. Phys.*, **30**, 839 (1959).

(5) J. Jortner, *Radiat. Res., Suppl.*, **4**, 24 (1964).

(6) K. Fueki, *J. Chem. Phys.*, **49**, 765 (1968).

(7) K. Fueki, D. F. Feng, and L. Kevan, *Chem. Phys. Lett.*, **4**, 313 (1969).

(8) K. Fueki, D. F. Feng, and L. Kevan, *J. Phys. Chem.*, **74**, 1976 (1970).

(9) K. Fueki, D. F. Feng, L. Kevan, and R. Christoffersen, *ibid.*, **75**, 2297 (1971).

(10) K. Fueki, D. F. Feng, and L. Kevan, *J. Chem. Phys.*, **56**, 5351 (1972).

(11) D. F. Feng, K. Fueki, and L. Kevan, *ibid.*, **57**, 1253 (1972).

(12) D. A. Copeland, N. R. Kestner, and J. Jortner, *ibid.*, **53**, 1189 (1970).

(13) R. A. Holroyd and M. Allen, *ibid.*, **54**, 5014 (1971).

(14) I. Eisele and L. Kevan, *ibid.*, **53**, 1867 (1970).

(15) T. Huang, I. Eisele, D. P. Lin, and L. Kevan, *ibid.*, **56**, 4702 (1972).

has established the photoconduction threshold for trapped electrons and other details of the energy level structure. This adds constraints for which a successful theoretical model must account. In this paper we extend the semicontinuum model to electrons in methyltetrahydrofuran (MTHF) and aliphatic amine glasses. It is particularly interesting that the rather complex experimentally determined energy level structure for electrons in MTHF[15] is predicted rather well by theory. The semicontinuum model has also been modified for trapped electrons in aqueous glasses like 10 *M* NaOH by neglecting long-range polarization interactions. This modification successfully predicts no bound excited state in agreement with experiment. In addition, our previous results on water and ice[9] are corrected and the effects of matrix polarity on the theoretical energy level structure of trapped electrons are critically discussed for all the matrices investigated to date.

Outline of Calculation

In the semicontinuum model of excess electrons in polar media the electron is considered to interact with a number N of specifically oriented matrix molecular dipoles in the first solvation shell by short-range attractive and repulsive potentials and with the rest of the matrix molecules beyond the first solvation shell by a long-range average polarization potential. The total energy of the excess electron in the medium is given by the sum of the electronic energy of the electron and the energy necessary to rearrange the medium due to its interaction with the electron.

The matrix dipoles in the first solvation shell are considered to be symmetrically arranged around the electron in a tetrahedral fashion for $N = 4$ and an octahedral fashion for $N = 6$. These dipoles are allowed to reach thermal equilibrium. Then for point depoles with dipole moment μ_0 and polarizability α, the electronic energy of the ith bound state for short-range attractive interactions is given by eq 1 where r_d is the distance be-

$$E_e^s(i) = -\int_0^{r_d} \Psi_i\left(\frac{Ne\mu_0\langle\cos\theta\rangle_{1s}}{r_d^2} + \frac{Ne^2\alpha C_i}{2r_d^4}\right)\Psi_i 4\pi r^2\,dr \quad (1)$$

tween the center of the electron charge distribution and the point dipole, θ is the angle between the dipole moment vector and the line joining the center of the electron charge distribution to the dipole, and C_i is the total charge density enclosed within radius r_d. The average value of cos θ as determined by temperature T and the local electric field E_{loc} is given by Langevin's relation $\langle\cos\theta\rangle_{1s} = \coth\chi - 1/\chi$ where $\chi = \mu_0 E_{loc}/kT$ and $E_{loc} = eC_{1s}/r_d^2$.

The short-range medium rearrangement energy associated with dipole orientation is a dipole–dipole repulsion term given by eq 2 where D_N is a numerical

$$E_m^s(i) = \frac{D_N}{r_d^3}\left(\mu_0\langle\cos\theta\rangle_{1s} + \frac{e\alpha C_i}{r_d^2}\right)^2 \quad (2)$$

constant calculated from the number and geometrical arrangement of the dipoles. Note that $E_m^s(i)$ depends on C_i so it must be determined self-consistently with the electronic energy.

(16) L. Kevan, *J. Phys. Chem.*, **76**, 3830 (1972).
(17) K. Kawabata, *J. Chem. Phys.*, **55**, 3672 (1971).

Another medium rearrangement energy term is E_v which is the energy required to form a void or cavity in the medium. E_v is given by $4\pi(r_d^2 - r_s^2)\gamma$ where γ is the surface energy and r_s is the radius of a matrix molecule. This energy contribution is generally small.

The short-range repulsion of the excess electron with the medium electrons is approximated by the quasi-free electron energy V_0 times the charge density outside r_d or $V_0(1 - C_i) = E_q$. V_0 is also the energy of the electron in the bottom of the conduction band state. V_0 has been approximately calculated for electrons in rare gases using a Wigner–Seitz or cell model, and although the approximate calculation cannot be readily extended to polar liquids V_0 is expected to be around zero.[12] In our calculation V_0 is taken to be a limited parameter and is chosen so that the calculated 1s → 2p transition energy fits reasonably well with the observed optical transition energy at the absorption maximum. The sensitivity of the results to V_0 is discussed in Results and Discussion, section IVD.

The medium beyond the first solvation shell beginning at $R = r_d + r_s$ is treated as a continuous dielectric characterized by static, D_s, and optical, D_{op}, dielectric constants. This long-range interaction consists of an electronic part E_e^l and a medium rearrangement part E_m^l due to the polarization of the dielectric medium. The electrostatic potential f_i is made self-consistent with the charge distribution of the excess electron $|\Psi_i|^2$ by solving Poisson's equation: $\nabla^2 f_i = 4\pi e|\Psi_i|^2$. The equations for the long-range interaction have been discussed previously for the ground and excited states.[9] The excited state is an unrelaxed nonequilibrium state consistent with the ground-state charge distribution due to Franck–Condon restrictions.

The total energy for the ith state is then given by

$$E_t(i) = E_k(i) + E_e^s(i) + E_m^s(i) + E_e^l(i) + E_m^l(i) + E_q(i) + E_v \quad (3)$$

where E_k is the kinetic energy of the excess electron. One parameter hydrogenic wave functions were used and the variational procedure was applied to the total energy of the system to obtain the minimum energy for a given r_d. This was repeated for various r_d to construct configuration coordinate curves.

The conduction state was treated as a delocalized unrelaxed state consistent with the ground-state charge distribution and is composed of the medium rearrangement energy terms plus V_0

$$E_t(\text{cond}) = E_m^s(\text{cond}) + E_m^l(\text{cond}) + E_v + V_0 \quad (4)$$

where $E_m^s(\text{cond}) = D_N\mu_0^2\langle\cos\theta\rangle_{1s}^2/r_d^3$ and

$$E_m^l(\text{cond}) = -\tfrac{1}{2}e(D_{op}^{-1} - D_s^{-1}) \times \left[f_{1s}(R)\int_0^R \Psi_{1s}^2 4\pi r^2\,dr + \int_R^\infty f_{1s}(r)\Psi_{1s}^2 4\pi r^2\,dr\right]$$

The expression for $E_m^l(\text{cond})$ has been corrected[10] from the original equation given in ref 9.

A minor programming error that affected the earlier results on water and ice[9] has been corrected and revised values are given here. The physical constants used in the calculations for the various matrices are listed in Table I.

Results and Discussion

The results of the calculations are given in Tables II–

Table I. Physical Constants of the Matrices

	T, °K	r_s, Å	μ_0, D	α, Å^3	D_s	D_{op}	γ, ergs/cm^2
Water	298	1.4[a]	1.85[c]	1.51[f]	80[c]	1.78[c]	72.0[c]
Ice	77	1.4	1.85	1.51	3.0[h]	1.78	100[l]
Methanol	298	1.6[b]	1.70[c]	3.23[f]	33.8[c]	1.77[c]	22.6[c]
Methanol	77	1.6	1.70	3.23	3.3[i]	1.77	45.2[m]
Ethanol	298	1.8[b]	1.69[c]	4.80[f]	24.3[c]	1.85[c]	22.3[c]
Ethanol	77	1.8	1.69	4.80	3.0[j]	1.85	44.6[m]
Methyltetrahydrofuran	77	2.0[b]	1.75[d]	7.90[g]	2.88[k]	2.00[c]	50.0[m]
2-Methyl-*n*-amylamine	77	2.5	1.10[e]	13.0	2.42	1.96	45.0
Diisopropylamine	77	2.5	0.85[e]	13.0	2.42	1.96	45.0
Triethylamine	77	2.5[b]	0.66[c]	13.0[g]	2.42[c]	1.96[c]	45.0[m]

[a] G. Némethy and H. A. Scheraga, *J. Chem. Phys.*, **36**, 3382 (1962). [b] Estimated values for the radius of the matrix molecule in the first solvation shell. [c] "Handbook of Chemistry and Physics," R. C. Weast, Ed., 50th ed, Chemical Rubber Publishing Co., Cleveland, Ohio, 1969. [d] Value for tetrahydrofuran from G. G. Engerholm, Ph.D. thesis; see *Diss. Abstr.*, **26**, 7060 (1966). [e] Values estimated from those of similar compounds.[c] [f] H. H. Landolt and R. Bornstein, "Zahlenwerte und Functionen," 6 Auflage, "Atom und Molecular Physik," 3 Teil, Springer-Verlag, Berlin, 1950, pp 509–517. [g] Values calculated from the Lorentz–Lorenz equation. [h] N. E. Dorsey, "Properties of Ordinary Water Substances in All Its Phases," Van Nostrand-Reinhold, Princeton, N. J., 1940, pp 485, 500. [i] D. J. Denney and R. H. Cole, *J. Chem. Phys.*, **23**, 1767 (1955). [j] Value estimated from that of solid methanol.[i] [k] K. F. Baverstock and P. J. Dyne, *Can. J. Chem.*, **48**, 2182 (1970). [l] N. H. Fletcher, "The Chemical Physics of Ice," Cambridge University Press, London, 1970, p 123. [m] Values taken to be twice as large as those of the corresponding liquids.[c]

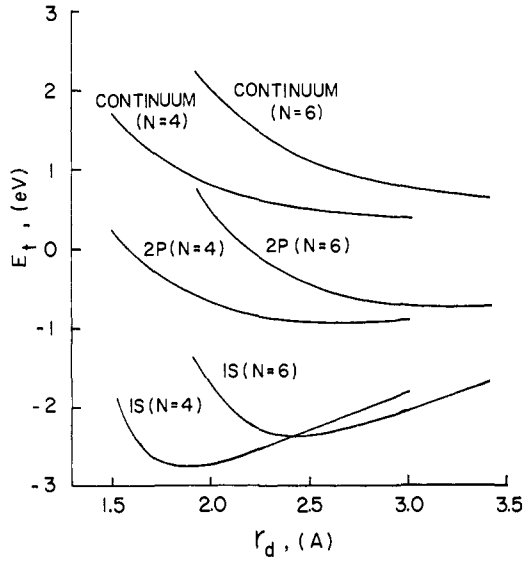

Figure 1. Configuration coordinate diagram for the solvated electron in water at 298 °K and $V_0 = -1.0$ eV.

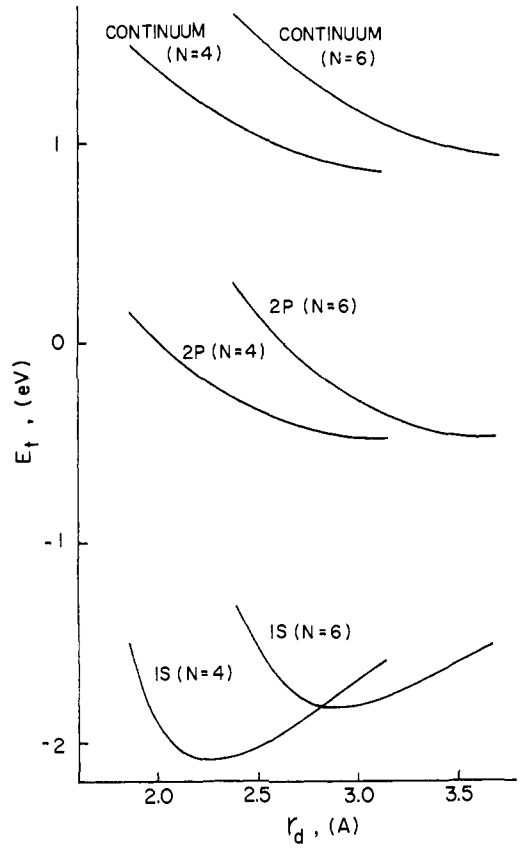

Figure 2. Configuration coordinate diagram for the solvated electron in methanol at 298 °K and $V_0 = -0.2$ eV.

V and Figures 1–9. The calculated properties of trapped electrons in various polar matrices are presented in Table II along with the experimental values. Here r_d^0 is the cavity radius at the configurational minimum, $h\nu$ is the 1s → 2p transition, I is the photoconductivity threshold energy, and ΔH is the heat of solution in which the energy required to break hydrogen bonds for electron solvation has been neglected. Table III shows various energy contributions to the total energy of trapped electrons in the 1s ground state. Table IV shows various energy contributions to the total energy of trapped electrons in the 2p excited state. Table V gives the charge distributions of trapped electrons in the ground and excited states. $C_i(r)$ is the fraction of charge enclosed within radius r for the trapped electron in the i state (i = 1s or 2p). The radii, r_v^0, r_d^0, and R_0 are the void radius, the cavity radius, and the first solvation shell radius at the configurational minimum, respectively.

I. Solvated Electrons in Polar Liquids. A. Water. Figure 1 shows configuration coordinate diagrams calculated for the solvated electron in water at 298 °K and $V_0 = -1.0$ eV. The configurational stability is established for the ground state at finite cavity radii for both $N = 4$ and 6. Figure 1 and Table II correct our previous results[9] on water.

In Table II are shown various properties of the solvated electron in water at 298 °K. The calculated 1s → 2p transition energies, $h\nu$, for $N = 4$ and 6 compare reasonably to the experimental $h\nu = 1.72$ eV[2] at the absorption maximum, although they somewhat overestimate the experimental value. The calculated oscil-

Table II. Properties of Trapped Electrons in Polar Matrices

Matrix	T, °K	V_0, eV	N	r_d^0, Å	$h\nu$, eV Calcd	$h\nu$, eV Obsd	f Calcd	f Obsd	I, eV Calcd	I, eV Obsd	ΔH, eV	θ, deg
Water	298	−1.0	4	1.93	2.15	1.72[a]	0.70	0.71[a]	3.63		2.75	14.1
			6	2.46	1.94		0.83		3.51		2.36	16.9
Methanol	298	−0.2	4	2.28	1.85	1.87[b]	0.71	0.78[a]	3.23		2.09	16.6
			6	2.92	1.56		0.86		3.03		1.83	20.4
Ethanol	298	0.2	4	2.54	1.79	1.80[b]	0.72	0.87[a]	3.10		1.77	17.9
			6	3.23	1.46		0.90		2.88		1.50	22.0
Ice	77	−1.0	4	1.93	1.84	1.9[c]	0.39	0.33[h]	2.36	2.3 ± 0.1[c]	2.08	7.2
			6	2.46	1.85		0.64		2.45		1.72	8.6
Methanol	77	0.5	4	2.32	2.09	2.3[d]	0.51	0.73[d]	2.73	2.4 ± 0.1[d]	1.33	8.3
			6	2.95	1.82		0.89		2.74		1.13	10.1
Ethanol	77	1.0	4	2.54	2.15	2.3[d]	0.58	0.66[d]	2.71	2.4 ± 0.1[i]	1.02	10.0
			6	3.28	1.70		0.94		2.70		0.80	10.0
2-Methyltetrahydrofuran	77	−0.5	4	2.87	1.04	1.0[e]	0.45	0.58[e]	1.42	1.6 ± 0.2[j]	1.35	10.3
			6	3.61	0.89		0.65		1.28		0.96	12.7
2-Methyl-*n*-amylamine	77	0.3	4	3.24	1.02	1.1[f]	0.35		1.28	(1.2 ± 0.1)[k]	0.66	14.1
Diisopropylamine	77	0.3	4	3.19	0.90	0.87[f]	0.36		1.16	1.0 ± 0.1[k]	0.57	16.0
Triethylamine	77	0.3	4	3.19	0.83	0.75[f]	0.37		1.08	0.9 ± 0.1[k]	0.50	18.3
Alkaline ice	77	0.0	4	2.04					1.04	1.5 ± 0.1[c]	0.30	7.4
			6	2.56					1.45		0.21	8.7

[a] E. J. Hart and M. Anbar, "The Hydrated Electron," Wiley-Interscience, New York, N. Y., 1970. [b] M. G. Robinson, K. N. Jha, and G. R. Freeman, *J. Chem. Phys.*, **55**, 4974 (1971). [c] K. Kawabata, *ibid.*, **55**, 3672 (1971); K. Ho and L. Kevan, unpublished work, see L. Kevan, *J. Phys. Chem.*, **76**, 3830 (1972). [d] A. Habersbergerová, L. Josimović, and J. Teplý, *Trans. Faraday Soc.*, 66, 656, 669 (1970). [e] T. Shida, *J. Phys. Chem.*, **73**, 4311 (1969). [f] S. Noda, K. Fueki, and Z. Kuri, *Chem. Phys. Lett.*, **8**, 407 (1971). [g] M. C. Sauer, Jr., S. Arai, and L. M. Dorfman, *J. Chem. Phys.*, **42**, 708 (1965). [h] G. Nilsson, H. Christensen, P. Pagsberg, and S. O. Nielsen, *J. Phys. Chem.*, 76, 1000 (1972). [i] A. Bernas, D. Grand, and C. Chachaty, *Chem. Commun.*, 1667 (1970). [j] T. Huang, I. Eisele, D. P. Lin, and L. Kevan, *J. Chem. Phys.*, **56**, 4702 (1972). [k] S. Noda, K. Fueki, and Z. Kuri, *Can. J. Chem.*, **50**, 2699 (1972).

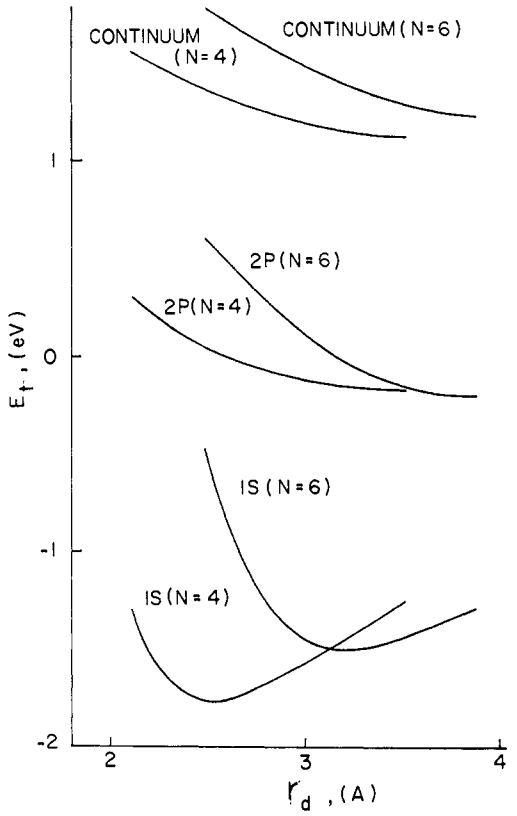

Figure 3. Configuration coordinate diagram for the solvated electron in ethanol at 298°K and $V_0 = 0.2$ eV.

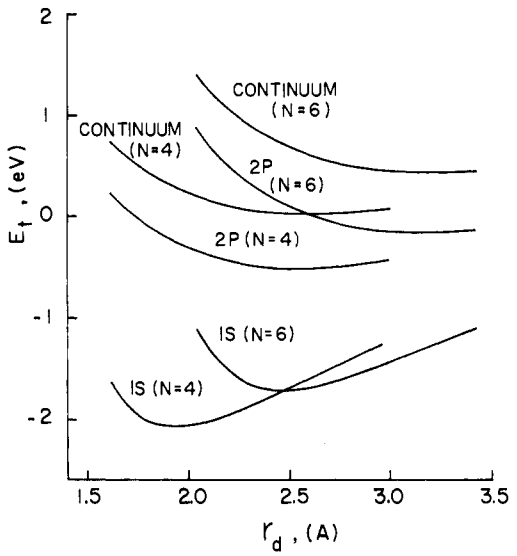

Figure 4. Configuration coordinate diagram for the trapped electron in ice at 77°K and $V_0 = -1.0$ eV.

lator strength, 0.70 for $N = 4$, is in good agreement with the experimental value, 0.71.[2] The calculated f for $N = 6$ is somewhat larger than the experimental value. The calculated threshold energy for photoconductivity, I, is considerably higher than the 1s → 2p transition energy. However, it has been suggested in a recent laser excitation study[18] that the optical absorption of the hydrated electron is possibly due to transitions to unbound excited states. The present calculations do not support this, and more direct experiments are needed to determine the nature of optical transitions of the hydrated electron. This is difficult in water, although in solid matrices it is possible to measure I.

The calculated values of ΔH are significantly higher than the experimental heat of solution, 1.7 eV.[2] At present there is no information on the possible energy for the hydrogen-bond rearrangement necessary to solvate the electron. If some of the hydrogen bonds are broken, then the calculated heat of solution, ΔH,

(18) G. Kenney-Wallace and D. C. Walker, *J. Chem. Phys.* **55**, 447 (1971).

Table III. Various Energy Contributions to the Total Energy of Trapped Electrons in the Ground State

Matrix	T, °K	N	E_k, eV	E_e^s, eV	E_m^s, eV	E_e^l, eV	E_m^l, eV	E_v, eV	E_q, eV	E_t, eV
Water	298	4	2.265	−4.326	1.687	−4.097	2.049	0.099	−0.429	−2.752
		6	1.744	−4.147	1.936	−3.546	1.773	0.231	−0.354	−2.364
Methanol	298	4	1.923	−3.691	1.450	−3.489	1.744	0.047	−0.074	−2.089
		6	1.402	−3.202	1.425	−2.996	1.498	0.106	−0.062	−1.830
Ethanol	298	4	1.783	−3.525	1.410	−3.115	1.558	0.056	0.065	−1.768
		6	1.282	−2.948	1.320	−2.684	1.342	0.126	0.056	−1.505
Ice	77	4	2.210	−4.323	1.716	−2.760	1.380	0.138	−0.437	−2.076
		6	1.724	−4.232	2.020	−2.392	1.196	0.320	−0.358	−1.721
Methanol	77	4	2.091	−3.928	1.488	−2.504	1.252	0.099	0.167	−1.334
		6	1.554	−3.472	1.509	−2.155	1.077	0.218	0.137	−1.131
Ethanol	77	4	1.996	−3.888	1.559	−2.178	1.089	0.112	0.290	−1.020
		6	1.428	−3.180	1.381	−1.859	0.930	0.263	0.879	−0.802
MTHF	77	4	1.299	−3.064	1.365	−1.881	0.941	0.166	−0.175	−1.349
		6	0.892	−2.527	1.289	−1.622	0.811	0.354	−0.161	−0.965
2-Methyl-*n*-amyl-amine	77	4	1.192	−2.526	1.156	−1.452	0.726	0.150	0.089	−0.664
Diisopropyl-amine	77	4	1.162	−2.346	1.111	−1.463	0.731	0.138	0.095	−0.573
Triethylamine	77	4	1.121	−2.130	0.999	−1.460	0.730	1.380	0.099	−0.504
Alkaline ice	77	4	2.232	−4.118	1.420	0.000	0.000	0.171	0.000	−0.295
		6	1.803	−4.130	1.758	0.000	0.000	0.362	0.000	−0.207

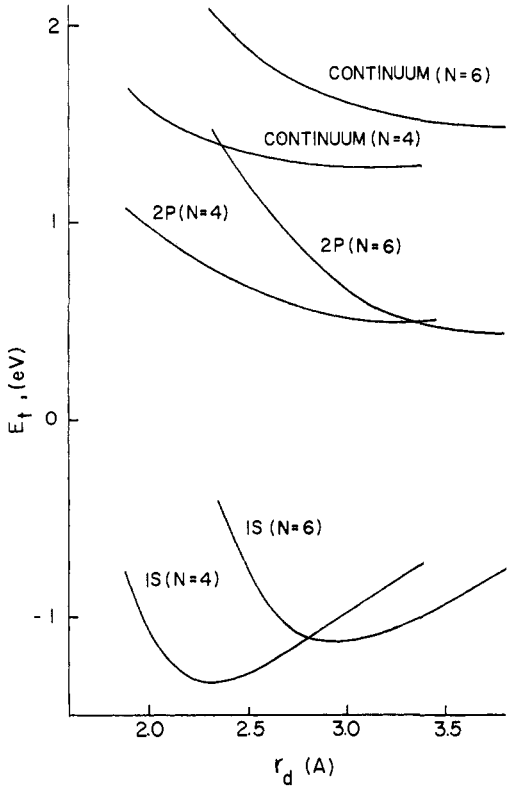

Figure 5. Configuration coordinate diagram for the trapped electron in methanol at 77°K and $V_0 = 0.5$ eV.

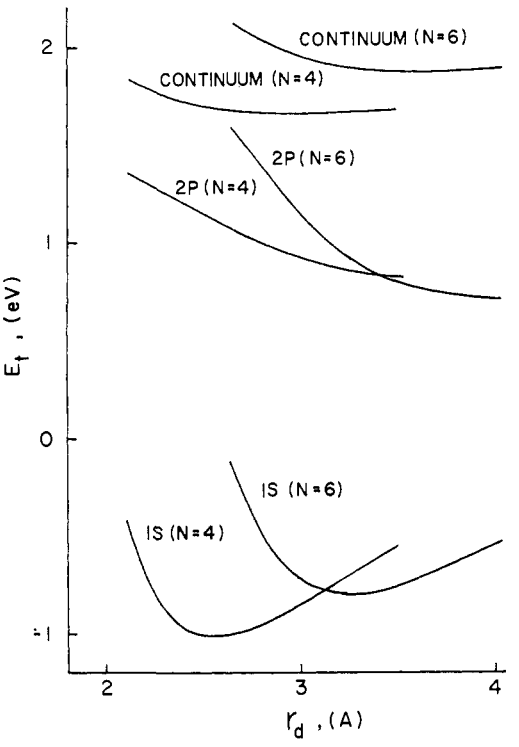

Figure 6. Configuration coordinate diagram for the trapped electron in ethanol at 77°K and $V_0 = 1.0$ eV.

would overestimate the experimental value. For example, if two hydrogen bonds are broken per molecule in the first solvation shell, the energy is 0.56 eV for $N = 4$ and 0.84 eV for $N = 6$.[19] The values of ΔH are then reduced to 2.19 eV for $N = 4$ and 1.52 eV for $N = 6$, which is in somewhat better agreement with experiment.

It can be seen in Table III that the short-range interactions, $E_e^s + E_m^s$, are more important than the long-range interactions, $E_e^l + E_m^l$, for stabilization of the solvated electron in the ground state. Also, it can be seen in Table IV that in contrast to the ground state, the long-range energy components contribute to the total energy of the solvated electron in the excited state much more than do the short-range energy components.

Table V shows that the fraction of charge enclosed within the first solvation shell radius, R_0, is ~90% for both $N = 4$ and 6 for the hydrated electron in the ground state, and ~30% for $N = 4$ and ~50% for $N = 6$ for the hydrated electron in the excited state. It should be noted that such charge distributions are related closely to the relative importance of the short- and long-range interactions mentioned above.

(19) G. Némethy and H. A. Scheraga, *J. Chem. Phys.* 36, 3382 (1962).

Table IV. Various Energy Contributions to the Total Energy of Trapped Electrons in the Excited State

Matrix	T, °K	N	E_k, eV	E_e^s, eV	E_m^s, eV	E_e^l, eV	E_m^l, eV	E_v, eV	E_q, eV	E_t, eV
Water	298	4	1.208	−0.417	0.743	−3.066	1.762	0.099	−0.930	−0.601
		6	1.491	−1.110	1.204	−3.075	1.636	0.231	−0.802	−0.426
Methanol	298	4	1.074	−0.405	0.442	−2.754	1.538	0.047	−0.180	−0.238
		6	1.307	−1.002	0.756	−2.696	1.410	0.106	−0.148	−0.266
Ethanol	298	4	1.059	−0.460	0.380	−2.588	1.403	0.056	0.173	0.024
		6	1.350	−1.142	0.710	−2.510	1.289	0.126	0.132	0.045
Ice	77	4	0.566	−0.107	0.698	−1.462	0.912	0.138	−0.982	−0.237
		6	0.963	−0.592	1.143	−1.772	0.962	0.320	−0.895	0.130
Methanol	77	4	0.823	−0.269	0.406	−1.755	0.983	0.099	0.466	0.755
		6	1.705	−1.486	0.923	−2.013	1.024	0.218	0.320	0.690
Ethanol	77	4	0.992	−0.425	0.386	−1.721	0.778	0.112	0.236	1.133
		6	1.873	−1.781	0.927	−1.801	0.795	0.263	0.513	0.900
MTHF	77	4	0.370	−0.094	0.216	−1.109	0.623	0.166	−0.482	−0.309
		6	0.461	−0.284	0.389	−1.180	0.626	0.354	−0.445	−0.079
2-Methyl-*n*-amyl-amine	77	4	0.290	−0.048	0.069	−0.864	0.468	0.150	0.289	0.354
Diisopropyl-amine	77	4	0.263	−0.030	0.043	−0.828	0.453	0.138	0.292	0.331
Triethylamine	77	4	0.252	−0.022	0.027	−0.812	0.446	0.138	0.292	0.322

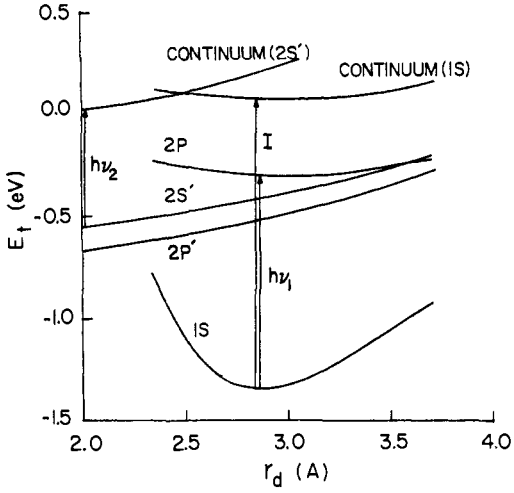

Figure 7. Configuration coordinate diagram for the trapped electron in MTHF at 77°K for $N = 4$ and $V_0 = -0.5$ eV.

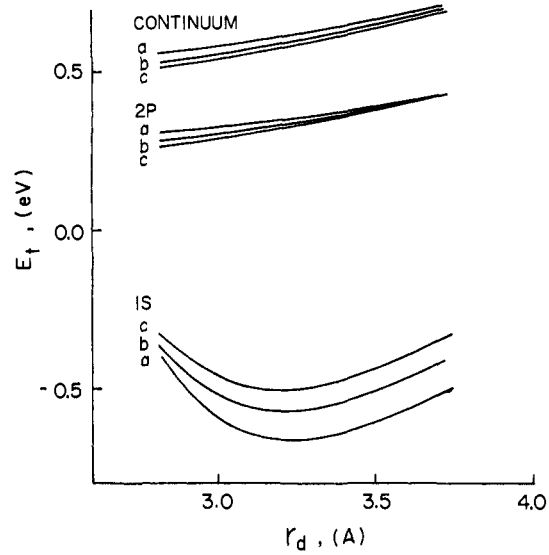

Figure 8. Configuration coordinate diagrams for the trapped electron in aliphatic amines at 77°K for $N = 4$ and $V_0 = 0.3$ eV: (a) 2-methyl-*n*-amylamine, (b) diisopropylamine, (c) triethylamine.

B. Methanol and Ethanol. Figures 2 and 3 show configuration coordinate diagrams for solvated electrons in methanol ($V_0 = -0.2$ eV) and ethanol ($V_0 = 0.2$ eV) at 298°K, respectively. Figure 2 corrects our previous result for methanol.[20]

As can be seen in Table II, the 1s → 2p transition energies and oscillator strengths calculated with these V_0 values are in excellent agreement with experiment. The calculated threshold energies for photoconductivity are significantly higher than the 1s → 2p transition energies for both $N = 4$ and 6; there are no available experimental data for comparison.

The cavity radius, r_d^0, for the solvated electron in methanol is smaller than that in ethanol and greater than that in water for the same N. The cavity radius for $N = 6$ is generally greater than that for $N = 4$ for the same solvent. The average angle, θ, of orientation of the solvent dipoles in the first solvation shell increases slightly from water to methanol to ethanol for the same N. The value of θ for $N = 6$ is somewhat greater than that for $N = 4$ for the same solvent. These trends in the values of θ arise from the fact that the electric field acting on the solvent dipoles is weaker for the dipoles at greater r_d^0, so θ is larger for larger r_d^0.

The various energy contributions to the total energies of solvated electrons in methanol and ethanol are similar to those in water except for E_q which depends on the value chosen for V_0.

The charge distributions for solvated electrons in methanol and ethanol are also similar to those in water, although the charge enclosed within a specified radius increases in the order of water, methanol, and ethanol for both the ground and excited states.

II. Trapped Electrons in Polar Solids. A. Ice. Figure 4 shows configuration coordinate diagrams for the trapped electron in ice at 77°K and $V_0 = -1.0$ eV and corrects our previous diagram for ice.[9] This diagram is similar to that for the solvated electron in water except that the difference in energy between the 2p state and the bottom of the continuum state is significantly smaller.

In Table II are given various properties of the trapped

(20) K. Fueki, D. F. Feng, and L. Kevan, *Chem. Phys. Lett.*, **10**, 504 (1971).

Table V. Charge Distributions of Trapped Electrons in Polar Matrices

Matrix	T, °K	N	Ground state $C_{1s}(r_v^0)$	Ground state $C_{1s}(r_d^0)$	Ground state $C_{1s}(R_o)$	Excited state $C_{2p}(r_v^0)$	Excited state $C_{2p}(r_d^0)$	Excited state $C_{2p}(R_o)$
Water	298	4	0.050	0.571	0.886	0.000	0.070	0.322
		6	0.174	0.646	0.893	0.011	0.198	0.529
Methanol	298	4	0.076	0.631	0.913	0.001	0.100	0.396
		6	0.218	0.688	0.911	0.021	0.260	0.610
Ethanol	298	4	0.083	0.675	0.935	0.001	0.134	0.482
		6	0.232	0.722	0.930	0.030	0.341	0.713
Ice	77	4	0.048	0.563	0.881	0.000	0.018	0.118
		6	0.172	0.642	0.891	0.005	0.105	0.348
Methanol	77	4	0.092	0.666	0.929	0.001	0.068	0.301
		6	0.250	0.726	0.929	0.037	0.361	0.727
Ethanol	77	4	0.094	0.710	0.949	0.001	0.121	0.454
		6	0.273	0.764	0.947	0.060	0.487	0.838
MTHF	77	4	0.083	0.650	0.922	0.000	0.036	0.191
		6	0.206	0.678	0.907	0.006	0.110	0.352
2-Methyl-*n*-amyl-amine	77	4	0.052	0.702	0.954	0.000	0.036	0.214
Diisopropyl-amine	77	4	0.042	0.683	0.949	0.000	0.028	0.183
Triethylamine	77	4	0.040	0.671	0.945	0.000	0.026	0.172
Alkaline ice	77	4	0.075	0.602	0.895	0.000	0.000	0.000
		6	0.217	0.684	0.909	0.000	0.000	0.000

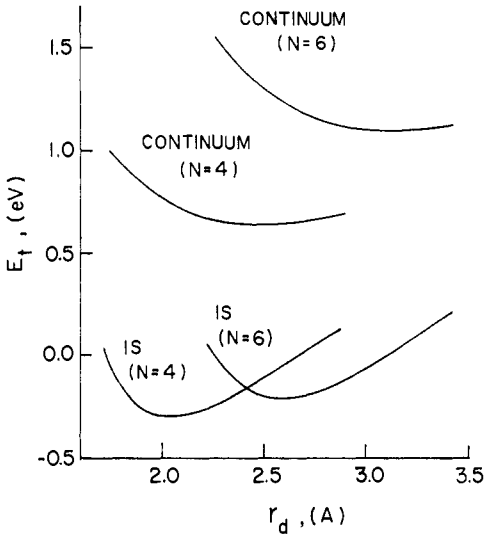

Figure 9. Configuration coordinate diagram for the trapped electron in 10 *M* NaOH glassy ice (alkaline ice) at 77°K and V_0 = 0.0 eV.

electron in ice at 77°K. The calculated 1s → 2p transition energies, oscillator strengths, and photoconductivity threshold energies are in good agreement with experiment. It is encouraging that the three observed optical properties of the trapped electron in ice can be well accounted for by the semicontinuum model.

The calculated values of ΔH for the trapped electron in ice are smaller than those for the solvated electron in water. This difference arises from the fact that the long-range electron-medium interactions are weaker in ice than in water (see Table III) because of the low static dielectric constant of ice at 77°K. The average angle of dipole orientation in the first solvation shell is significantly smaller in ice at 77°K than in water at 298°K because of the large difference in temperature.

General trends in various energy contributions to the total energies of the trapped electron in ice in the ground and excited states are similar to those of the solvated electron in water. However, the short-range interactions are much more important than the long-range interactions for the trapped electron in ice in the ground state. The difference in energy between the 2p excited state and the bottom of the continuum state is much smaller for the trapped electron in ice than for the solvated electron in water. This difference arises from the fact that the long-range interactions in the excited state are much weaker for the trapped electron in ice than for the solvated electron in water (see Table IV) because of the low static dielectric constant of ice at 77°K.

The calculated charge distributions of the trapped electron in ice in its ground state are very similar to those of the solvated electron in water, but the charge distributions of the excited state are significantly broader for the trapped electron in ice than for the solvated electron in water (see Table V).

B. Methanol and Ethanol. Figures 5 and 6 show configuration coordinate diagrams for trapped electrons in glassy methanol (V_0 = 0.5 eV) and ethanol (V_0 = 1.0 eV) at 77°K. These diagrams are similar to configuration coordinate diagrams for solvated electrons in liquid methanol and ethanol except that the difference in energy between the 2p state and the bottom of the continuum state is significantly smaller for trapped electrons in glassy alcohols. To obtain reasonable agreement between the calculated 1s → 2p and observed transition energies, it is necessary to assume higher values of V_0 for glassy alcohols than are assumed for liquid alcohols. This is understandable because of the difference in medium density between glassy alcohols and liquid alcohols. V_0 tends to increase with increase in medium density as shown in a previous paper.[11] The calculated results for the trapped electron in glassy ethanol have been obtained with the angle of dipole orientation in the first solvation shell fixed at 10°. The effects of dipole orientation at various angles on the properties of the trapped electron in glassy ethanol were fully discussed in a previous paper.[10]

The calculated 1s → 2p transition energies and oscillator strengths are in reasonable agreement with

experiment. The calculated threshold energies for photoconductivity are about 2.7 eV for both methanol and ethanol and for both $N = 4$ and 6. Although this value is somewhat higher than the experimental value of about 2.4 eV,[21,22] it is perhaps more significant to discuss $I - h\nu$. The calculated values of $I - h\nu$ are $\sim$0.6 eV while the experimental values are $\sim$0.1 eV. It is possible that this disagreement is partly due to a distribution of electron-trap depths which could result in a distribution of photoconductivity threshold energies, but we will see the calculated value of $I - h\nu$ for trapped electrons in MTHF is in better agreement with the experimental values.

The values of ΔH are considerably smaller for electrons in the glasses *vs.* the liquids. This again arises from the difference in the energy contribution of the long-range interactions and also from the difference in the values of V_0.

General trends in the various energy contributions and in the charge distributions of electrons in glassy alcohols *vs.* liquid alcohols are similar to the trends for electrons in water and ice for the same reasons given above.

C. Methyltetrahydrofuran (MTHF). Figure 7 shows configuration coordinate diagrams for trapped electrons in glassy MTHF at 77°K ($N = 4$ and $V_0 = -0.5$ eV). In Figure 7, in addition to the 1s state, the unrelaxed 2p state, and the continuum state corresponding to the 1s state, configuration coordinate curves of the relaxed 2s and 2p states, and the continuum state corresponding to the relaxed 2s state are also shown as 2s′, 2p′, and continuum (2s′). The procedures for calculating these relaxed states were outlined previously.[9]

It can be seen in Figure 7 that the configurational stability of the 1s ground state is established at a finite cavity radius and that the energies, E_t, of the 2p state and the bottom of the continuum (1s) state do not vary very much with the change in the configuration coordinate or cavity radius, r_d. The energies of the relaxed 2s and 2p states and the bottom of the continuum (2s′) state increase gradually with increase in r_d. It can also be seen that the relaxed 2s state lies above the relaxed 2p state by about 0.1 eV all along the configuration coordinate and the relaxed 2s crosses the unrelaxed 2p state at an energy coordinate close to its configurational minimum energy.

The relaxed states in MTHF were calculated in order to compare with the rather complex energy level structure deduced by experiment for e_t^- in MTHF.[15] Not only were transitions to a bound excited state ($h\nu_1$) and to the continuum (I) found, but also a two photon path to the continuum *via* a relaxed excited state was deduced. The theoretical results in Figure 7 certainly support this two photon pathway *via* $h\nu_1$, relaxation to the 2s′ state, and $h\nu_2$ to the continuum. The 2s′ continuum level simply corresponds to Franck–Condon vertical transitions from the 2s′ state.

In Table II are given the calculated properties of trapped electrons in MTHF at 77°K for $N = 4$ and 6 together with the experimental values. The agreement is generally good. The calculated energy difference between the relaxed 2s state and the bottom of the continuum state (2s′) is 0.6 eV, which is only in fair agreement with the observed value 1.1 eV,[15] but the qualitative significance of this calculated transition is very important.

Various energy contributions to the total energies of trapped electrons in glassy MTHF are given in Tables III and IV. The short-range interactions are much more important than the long-range interactions for the trapped electrons in the ground state, whereas the long-range interactions are predominant for the excited state. The charge distributions of the trapped electrons are given in Table V.

D. Aliphatic Amines. Figure 8 shows configuration coordinate diagrams for trapped electrons in glassy 2-methyl-*n*-amylamine (curve a), diisopropylamine (curve b), and triethylamine (curve c) at 77°K for $N = 4$ and $V_0 = 0.3$ eV. The configurational stability is established for the ground state in each case. The energies of the 2p state and the continuum state increase with increasing cavity radius and no minimum is observed. In all other, more polar, systems minima have been observed in these excited states. It is interesting to note that the 1s ground-state energy is in increasing order for curves a, b, and c, whereas the 2p excited-state energy and the energy of the bottom of the continuum state are in decreasing order for curves a, b, and c.

In Table II, the calculated 1s → 2p transition energies, $h\nu$, and the photoconductivity threshold energies, I, are in reasonable agreement with the observed values.[23,24] Since the value of I for 2-methyl-*n*-amylamine is not available, the calculated I for this amine is compared with the value of I for *sec*-butylamine which has an optical absorption spectrum similar to that of 2-methyl-*n*-amylamine. It is rather intesting that $I - h\nu = 0.26$ eV for all of these amines. This occurs because the excited state and continuum levels are affected equally by changing the dipole moment.

The matrix parameters for the amine glasses are all identical except for the dipole moment. Yet the trend in experimental $h\nu$ values is exactly reproduced by the calculated $h\nu$ values. We regard this as a major success of the semicontinuum model, particularly as regards the incorporation of short-range interactions.

The calculated oscillator strengths for the 1s → 2p transition seem rather low but no experimental values exist for comparison. The calculated values of ΔH decrease and the values of θ increase from 2-methyl-*n*-amylamine to diisopropylamine to triethylamine. It is reasonable that the calculated cavity radii are about the same for all of these amines.

The fraction of charge enclosed within the first solvation shell radius is about 95% for the ground state, and about 20% for the excited state. Such very diffuse charge distributions in the excited state together with the small permanent dipole moments are responsible for the characteristic shape of the configuration coordinate curves for the excited state of trapped electrons in these amines.

III. Trapped Electrons in 10 *M* NaOH Glassy Ice. The first glassy matrix in which trapped electrons were discovered was 10 *M* NaOH ice (alkaline ice) at 77°K.[25]

(21) A. Habersbergerova, L. Josimovic, and J. Teply, *Trans. Faraday Soc.*, **66**, 656, 669 (1970).
(22) A. Bernas, D. Grand, and C. Chachaty, *Chem. Commun.*, 1667 (1970).
(23) S. Noda, K. Fueki, and Z. Kuri, *Chem. Phys. Lett.*, **8**, 407 (1971).
(24) S. Noda, K. Fueki, and Z. Kuri, *Can. J. Chem.*, 50, 000 (1972).
(25) D. Schulte-Frohlinde and K. Eiben, *Z. Naturforsch. A*, 17, 445 (1972); *ibid.*, **18**, 199 (1963).

Electrons can also be trapped in other glassy ices containing large amounts of solutes.[3a] Although we do not know the various physical constants for these highly doped glassy ice matrices, it does seem that the high ion concentration will dominate the water dipole orientation beyond the first solvation shell around a trapped electron. In other words almost all of the water molecules are oriented around the ions in the matrix and when an excess electron is produced its field is only effective on its first solvation shell of water molecules. We assume that water molecules beyond this first solvation shell are not significantly reoriented by the field of the excess trapped electron. We also assume that any net effect of the positive and negative ions in the matrix at the trapped electron averages to zero. Therefore, we will neglect the long-range polarization interactions but will still use the properties of ice in treating trapped electrons in alkaline ice. Figure 9 gives the configuration coordinate diagram. The new feature is that no stable bound excited state exists. In fact, the energy of the 2p excited state becomes identical with the energy of the continuum state. The total energy of the 2p and continuum states is given by eq 3 and 4. In the absence of long-range polarization interactions E_e^l and E_m^l are zero. It is also found that the charge distribution of the 2p state is so diffuse that $C_{2p} \sim 0$. Consequently $E_k = E_c^s \sim 0$. Since $E^s_m(2p) \sim E_m^s(\text{cond})$, we find that $E_t(2p) \sim E_t(\text{cond}) = E^s_m(\text{cond}) + V_0 + E_v$.

Figure 9 shows that the configurational stability of the 1s ground state is established. The calculated properties of the trapped electrons are given in Table II, and the various energy contributions and charge distributions are given in Tables III and V. Since no bound excited state is predicted, I but not $h\nu$ appears in Table II. For $V_0 = 0.0$ eV, $I = 1.04$ eV for $N = 4$ and 1.45 eV for $N = 6$. Experimentally, it has been shown that no bound excited state does exist for trapped electrons in alkaline ice.[14,26] The onset of the absorption band then gives I and has been estimated as 1.5 eV.[16] This is in reasonable agreement with the calculated values. It thus appears that we have successfully adapted the semicontinuum model to aqueous glasses containing large quantities of dissolved salts.

IV. Effects of Matrix Properties on the Properties of Trapped Electrons. Since the calculated properties of trapped electrons in various matrices are generally affected by several of the matrix properties summarized in Table I, it is not so simple to describe separately the way that each of these properties affects the properties of the trapped electrons. Nevertheless, such general comments are extremely useful from an experimental point of view and are attempted here. The energies of trapped electrons are rather insensitive to the values of γ because the surface energy term is small and to D_{op} because it does not vary much between matrices. The energies are also largely insensitive to r_s within a few tenths of an Ångström so the estimations used in some cases for r_s are not critical. The other matrix properties are of more importance and are discussed separately.

A. Permanent Dipole Moment. The permanent dipole moment of the matrix molecule contributes to the orientational polarization energy of the molecules in the first solvation shell. This orientational polarization energy increases in its magnitude with increase of the permanent dipole moment. As a result, the optical transition energy and the photoconductivity threshold energy increase with increase in the permanent dipole moment. This is seen when these properties of trapped electrons in glassy amines are compared with those in ice, glassy methanol, and ethanol. The permanent dipole moment also contributes to the short-range medium rearrangement energy by the dipole–dipole repulsion between the oriented dipoles in the first solvation shell. This interaction partially cancels the short-range attractive interaction.

The clearest effect of changing the dipole moment alone is illustrated by the amine results in which all matrix properties, except the dipole moment, and V_0 are the same. Both $h\nu$ and I increase with the dipole moment, but the fractional changes in $h\nu$ and I are smaller than those in the dipole moments. Figure 8 also shows that increased dipole moment stabilizes the ground state but destabilizes the first excited and continuum states. However, the effect on the ground state predominates.

Among ice, methanol glass, ethanol glass, and MTHF glass, the dipole moment is not the controlling factor for determining $h\nu$ or I. Also V_0 is not taken as the same for these matrices and this obscures the relatively small effect of the dipole moment on the energy levels.

B. Polarizability. The molecular polarizability of the matrix molecule contributes to the electronic polarization energy of the molecules in the first solvation shell. The polarizability is also related to the short-range medium rearrangement energy, since the polarizability is included in the effective dipole moment as the induced dipole moment. So, increasing polarizability is expected to have similar effects to increasing dipole moment, if all other matrix properties and V_0 are held constant. If the magnitude of the permanent dipole moment is about the same, there is an empirical, but not causative, trend between polarizability and V_0. This apparent trend can be seen for the solvated electrons in water, liquid methanol, and ethanol, and for the trapped electrons in ice, glassy methanol, and ethanol. Although MTHF has a rather large polarizability, it was necessary to assume a lower value of V_0 in MTHF than expected from the above trend to account for the low optical transition energy of trapped electrons in MTHF.

C. Static Dielectric Constant. The static dielectric constant of the matrix contributes to the long-range orientation polarization energy of the continuous dielectric medium. But it does not make a significant difference in the energy levels of solvated electrons in different polar liquids, because D_s appears in the factor $[(1/D_{op}) - (1/D_s)]$ and $D_{op} \ll D_s$. The static dielectric constant at 77°K is very similar in the different glassy matrices so again it does not affect the energy levels strongly. However, D_s does dominate the effects on the electron energy levels in liquids compared with 77°K solids. The main effect is to lower I by about 0.8 eV on going from liquid to solid. Thus the semicontinuum model predicts that the excited state is rather strongly bound with respect to the continuum state for solvated electrons in liquids. No direct experimental evidence yet bears on this point, but hopefully some will be

(26) P. Hamlet and L. Kevan, *J. Amer. Chem. Soc.*, **93**, 1102 (1971).

forthcoming. Since I for trapped electrons in solids, for which there is experimental information, is predicted fairly well by the semicontinuum model, the determination of I for electrons in liquids would be a critical test. If I turns out to be low for electrons in liquids, it would imply that short-range interactions are even more important than so far incorporated in the theory.

D. Energy of the Continuum Electron State. The energy of the continuum electron state, V_0, is largely due to a balance between polarization forces, which give a negative contribution, and electron–molecule repulsion, which gives a positive contribution.[12] At present, it is too difficult to evaluate V_0 theoretically for molecular systems; and experimental determination, although probably possible in polar media,[13] has not yet been done. So, in the semicontinuum model, V_0 has been treated as a limited (to ± 1 eV) adjustable parameter. We have shown previously[9,10] that an increase in V_0 in the same matrix increases $h\nu$ and decreases ΔH.

The values of V_0 used to give fits to experimental $h\nu$ values do not appear to indicate any general correlation with matrix properties. It is noted that for water, methanol, and ethanol in both liquid and solid phases, V_0 becomes more positive with increasing polarizability. This is opposite to expectation since polarization forces are thought to give a negative contribution to V_0. On the other hand V_0 becomes more positive as the density increases from liquid to solid methanol and ethanol. This does agree with expectation since electron–molecule repulsion increases with density.

One can ask whether the values of V_0 which give agreement with the experimental $h\nu$ values seem reasonable. In liquid alkanes, photoemission experiments have given V_0 values from -0.4 to 0.0 eV which roughly are given by $V_0 \sim E^* - 8.4$ eV where E^* is the lowest electronic state of the molecule vapor.[13] It is probably doubtful whether this rough correlation extends to polar liquids and solids, but, if so, it would predict $V_0 \sim -1.0$ eV for H_2O, or $V_0 \sim -1.3$ eV for methanol and ethanol and $V_0 \sim -1.1$ eV for tetrahydrofuran. There is no clear predicted trend with matrix polarity, although the estimated V_0 values are all negative. In the absence of experimental data, we believe the V_0 values in Table II are reasonable, except perhaps for positive values above $+0.2$ to 0.3 eV.

With regard to matrix properties, it should be noted that ethanol glass and MTHF glass are rather similar except for V_0. The difference in calculated $h\nu$ values in these two matrices is largely due to the difference in V_0.

E. General Comments. We may consider the solid matrices to decrease in general polarity in the order ice, methanol, ethanol, MTHF, 2-methyl-*n*-amylamine, diisopropylamine, and triethylamine. The values of $h\nu$ generally decrease with decreasing polarity, except for ice. This trend is generally reproduced by the semicontinuum model. The value of I also generally decreases with polarity, but the quantity $I - h\nu$ is perhaps more significant. $I - h\nu$ represents the stabilization of the first excited state with respect to the conduction state, and this energy generally decreases with decreasing polarity, $I - h\nu$ averages 0.57 eV for ice and alcohols, 0.38 eV for MTHF, and 0.26 eV for amine glasses. In contrast, $I - h\nu = 0$ for trapped electrons in 10 M NaOH glassy ice which must be regarded as highly polar. This occurs because the long-range polarization interactions are rendered ineffective by the ions in this matrix. So, as far as trends go, the alkaline ice matrix is in a different class from the pure matrices.

The value of r_d^0 may be regarded as a rough measure of the size of the electron wavefunction. In recent electron–nuclear double resonance experiments[27] we have shown that experimental values of the size of the trapped electron wavefunction in several glassy matrices are in approximate agreement with the r_d^0 values. The r_d^0 values increase with decreasing polarity but this does not necessarily mean that the electron cavity size is increasing. Recall that $r_d^0 = r_s + r_v^0$ where r_s is the radius of the matrix molecules. Then r_v^0 is the electron void radius. We find that r_v^0 is reasonably constant for the seven matrices studied and equals 0.71 ± 0.06 Å with extremes of 0.53 Å for ice and 0.87 Å for MTHF. It is also worth noting that r_d^0 and r_v^0 are insensitive to changes in V_0 and phase (liquid to solid which changes D_s) in the same matrix.

In this paper, the semicontinuum model has been extended over about as wide a range of matrix polarity as applicable and has also been modified to apply to aqueous glasses containing high salt concentrations. We cannot extend this model to electron trapping in nominally nonpolar hydrocarbons because μ_0 and $D_s - D_{op}$ became too small to establish configurational stability of the ground state. Of course, electrons are trapped in alkane glasses.[3b] We feel that this must be associated with local C–H bond dipole moments rather than with the molecular dipole moments used in the semicontinuum model. A microdipole model invoking the bond dipole moment concept is currently being developed and appears to qualitatively account for electron trapping in alkane glasses.[28]

Acknowledgment. This research was supported by the U. S. Atomic Energy Commission under Contract AT(11-1)-2086 and by the Computing Center at Wayne State University. K. F. was supported by the Air Force Office of Scientific Research under Grant AFOSR-70-1852.

(27) J. Helbert, B. Bales, and L. Kevan, *J. Chem. Phys.*, **57**, 723 (1972).

(28) H. Yoshida, D. F. Feng, and L. Kevan, unpublished results.